Equilibrium microstates which generate second law violating steady states

Denis J. Evans and Debra J. Searles

Research School of Chemistry, The Australian National University, Canberra, Australian Capital Territory 0200, Australia

For reversible deterministic N-particle thermostatted systems, we examine the question of why it is so difficult to find initial microstates that will, at long times under the influence of an external dissipative field and a thermostat, lead to second law violating nonequilibrium steady states. We prove that the measure of those phases that generate second law violating phase space trajectories vanishes exponentially with time.

For reversible deterministic N-particle thermostatted systems, we examine the question of why it is so difficult to find initial microstates that will, at long times, under the application of an external dissipative field, lead to second law violating nonequilbirum steady states. In *reversible* systems, for each second law satisfying trajectory there is by definition a second law violating *antitrajectory* [1]. It is also known that antitrajectories are less stable mechanically than their conjugate second law satisfying trajectories [1,2]. It might appear that microscopic mechanical stability thus provides an explanation for the validity of the second law. We show, however, that this argument is not directly relevant to the validity of the second law.

When trajectories are followed essentially exactly and mechanical instabilities have not yet become large enough to have observable consequences on system dynamics, second law satisfying trajectories are still observed overwhelmingly often. We show that the second law is observed overwhelmingly often because at *equilibrium*, the measure of those initial states that subsequently lead to second law violating trajectories vanishes exponentially with respect to the time over which these violations occur.

To save space we discuss these matters with reference to thermostatted planar Couette flow. Analogous arguments and conclusions can be given for other transport processes. Thermostatted electrical conduction is comparatively simple.

We assume that at $t=0$, the initial phase $\Gamma=(x_i,y_i,z_i,p_{xi},p_{yi},p_{zi}; i=1,\ldots,N)$ of an N-particle system occurs with a probability given by the microcanonical distribution, which is a function of the equilibrium Hamiltonian of the system $H_0=\sum_{i=1}^N p_i^2/2m +\Phi$, where $\Phi(x_i,y_i,z_i; i=1,\ldots,N)$ is the potential energy. At $t=0$ a dissipative external field, F_e is applied to the system. This field does work on the system [1] $dH_0/dt \equiv -J(\Gamma)F_e$, where $-J(\Gamma)$, a phase function, is called the dissipative flux. However, the system is thermostatted (see below), enabling it to relax to a nonequilibrium steady state in a characteristic time which can be chosen to be, say, two Maxwell times [1] $2\tau_M$. In the language of statistical mechanics, the distribution function that characterizes the ensemble of systems changes under the combined influence of the external field and the

thermostat from the initial equilibrium distribution, through time varying transient distributions to the steady state distribution function at times $t \gg \tau_M$.

Because the initial equilibrium distribution is an even function of the particle momenta $\mathbf{p}_i=(p_{xi},p_{yi},p_{zi})$ and Hamilton's equations of motion are reversible, the equilibrium ratio of probabilities of observing any phase space trajectory segment $\Gamma(t;t_0 \to t_1) \equiv \Gamma_{(i)}$ and its time reversed antisegment $\Gamma(t;t_1 \to t_0) \equiv \Gamma_{(i*)}$ is unity $\mu_{i*}/\mu_i=1$. If we adopt the convention that away from equilibrium a trajectory segment has a positive average entropy production over the time span $t_1-t_0 \equiv \tau$, then by definition the corresponding antisegment has a negative average entropy production and is therefore forbidden macroscopically according to the second law of thermodynamics. In this paper we explore the temporal evolution of the anisotropy in the probability of observing segments and their conjugate antisegments for reversible deterministic systems.

We recently developed [2] a natural invariant measure [3] which enabled us to derive an expression for the ratio of probabilities of finding a fluid on a phase space trajectory segment of duration τ, in a nonequilibrium steady state with a dissipative flux $-J$, in the direction of, or opposite to, the imposed external force F_e. The second case would constitute for the entire trajectory $\tau \to \infty$, a violation of the second law of thermodynamics.

For sufficiently large τ, the normalized natural invariant measure that we introduced for multidimensional systems was [2]

$$\mu_i = \frac{\exp\left[-\sum_{n|\lambda_{ni}>0} \lambda_{ni}\tau\right]}{\sum_j \exp\left[-\sum_{m|\lambda_{mj}>0} \lambda_{mj}\tau\right]}, \tag{1}$$

where $\{\lambda_{ni}; n=1,\ldots,6N\}$ is the set of local Lyapunov exponents [4] for segment i. The sums appearing in (1) are carried out only over the expanding Lyapunov exponents for each segment i.

Now the ratio of the limiting $(\tau \to \infty)$ probabilities that the system is on a segment i and its conjugate antisegment $i*$ is

$$\frac{\mu_{i\ast}}{\mu_i} = \frac{\exp\left[-\sum_{n|\lambda_{ni\ast}>0}\lambda_{ni\ast}\tau\right]}{\exp\left[-\sum_{m|\lambda_{mi}>0}\lambda_{mi}\tau\right]}$$

$$= \frac{\exp\left[\sum_{n|\lambda_{ni}>0}\lambda_{ni}\tau\right]}{\exp\left[-\sum_{m|\lambda_{mi}<0}\lambda_{mi}\tau\right]}$$

$$=\exp\left[\tau\sum_n\lambda_{ni}\right]=\exp[-3N\langle\alpha\rangle_{\tau i}\tau] , \tag{2}$$

where we used that [1]

$$3N\langle\alpha\rangle_{\tau i}=-\sum_{i=1}^{6N}\lambda_{ni} . \tag{3}$$

We emphasize that (2) involves the sum of all the exponents for segment i which, as is shown below, is related to the heat removed per unit time by the thermostat in order to maintain a steady state [1].

One might assume that the decrease in the ratio $\mu_{i\ast}/\mu_i$ from its equilibrium value of unity to its steady state value of zero is a direct result of the fact that antisegments are less stable mechanically than their corresponding segments. This is certainly true. Both the largest Lyapunov exponent and the sum of the expanding Lyapunov exponents are observed [1,2] to be larger for antisegments than for segments. Therefore in any imperfect integration of the equations of motion, the system will, because of error and/or noise propagation, eventually follow the more stable class of trajectories, namely, the second law satisfying segments.

However, from nonlinear response theory [1] we have the exact result for the initial transient response of, say, the ensemble averaged dissipative flux to a step function external field $F_e(t)=F_e\Theta(t)$ that [1]

$$\lim_{t\to0}\langle J(t)\rangle=-\beta F_e t\langle J^2(0)\rangle<0 , \tag{4}$$

where $\beta=1/k_BT$, k_B is Boltzmann's constant, and T is the $t=0$ *equilibrium* absolute temperature. This result is exact for arbitrary F_e and is derived assuming that the equations of motion are solved *exactly*. The fact that the $t=0^+$ response immediately assumes a sign which is consistent with the second law of thermodynamics means that the relative mechanical stability of segments and their conjugates plays no role here.

We now discuss these processes in more detail for a thermostatted system of N particles under shear. Thus the external field is the shear rate $\partial u_x/\partial y=\gamma$, the gradient in the y direction of the x-streaming velocity, and the shear stress $-P_{xy}$ times the system volume V is the dissipative flux $-J$ [1]. The equations of motion for particles in such a system are the so-called thermostatted Sllod equations [1] (so called because of their close relationship to the Dolls tensor algorithm)

$$\dot{\mathbf{q}}_i=\mathbf{p}_i/m +i\gamma y_i , \quad \dot{\mathbf{p}}_i=\mathbf{F}_i-i\gamma p_{yi}-\alpha\mathbf{p}_i . \tag{5}$$

At low Reynolds number the momenta $\mathbf{p}_i$ are peculiar moment and α is determined using Gauss's principle of least constraint to keep the internal energy fixed [1]. Thus

$$\alpha=-\gamma\left[\sum_{i=1}^{N}p_{xi}p_{yi}\Big/m -\tfrac{1}{2}\sum_{i,j}x_{ij}F_{yij}\right]\Big/\left[\sum_{i=1}^{N}\mathbf{p}_i^2\Big/m\right]$$

$$=-P_{xy}\gamma V\Big/\left[\sum_{i=1}^{N}\mathbf{p}_i^2\Big/m\right] , \tag{6}$$

where F_{yij} is the y component of the intermolecular force exerted on particle i by j and $x_{ij}=x_j-x_i$. Therefore (3) gives the generalized entropy production per unit time [1]. We note that the equations of motion (5) and (6) are time reversible [1].

We have proved [1] that for every i segment with τ-averaged current $\langle P_{xy}\rangle_{\tau,(i)}$, $\equiv(1/\tau)\int_0^\tau P_{xy}(\Gamma_{(k)}(s))ds$, there exists a conjugate segment which we will call the $i^{(K)}$ segment for which $\langle P_{xy}\rangle_{\tau,(i^{(K)})}=-\langle P_{xy}\rangle_{\tau,(i)}$. The K mapping of a phase Γ is defined by $M^K\Gamma=M^K(x,y,z,p_x,p_y,p_z,\gamma)=(x,-y,z,-p_x,p_y,-p_z,\gamma)\equiv\Gamma^{(K)}$ [1]. It is straightforward to show that the Liouville operator for the system (5) and (6) $iL(\Gamma,\gamma)\equiv\sum[\dot{\mathbf{q}}_i\cdot\partial/\partial\mathbf{q}_i+\dot{\mathbf{p}}_i\cdot\partial/\partial\mathbf{p}_i]$ has the property that under a K map, $M^KiL(\Gamma,\gamma)=iL(\Gamma^{(K)},\gamma)=-iL(\Gamma,\gamma)$, from which it follows that [1]

$$P_{xy}(-t,\Gamma,\gamma)=\exp[-iL(\Gamma,\gamma)t]P_{xy}(\Gamma)$$

$$=-P_{xy}(t,\Gamma^{(K)},\gamma) . \tag{7}$$

We will now describe how to construct, from an arbitrary phase space trajectory segment i, its conjugate segment $i^{(K)}$. From this construction we will be able to deduce the time dependent ratio $\mu_{i^{(K)}}(\tau)/\mu_i(\tau)$ and understand why as τ increases, it becomes progressively more difficult to observe antisegments rather than segments.

If we select an initial $t=0$ phase $\Gamma_{(1)}$ and we advance time from 0 to τ using the equations of motion (5) and (6) we obtain $\Gamma_{(2)}=\Gamma(\tau;\Gamma_{(1)})=\exp[iL(\Gamma_{(1)},\gamma)\tau]\Gamma_{(1)}$. Continuing on to 2τ gives $\Gamma_{(3)}=\exp[iL(\Gamma_{(2)},\gamma)\tau]\Gamma_{(2)}=\exp[iL(\Gamma_{(1)},\gamma)2\tau]\Gamma_{(1)}$.

At the *midpoint* of the trajectory segment $\Gamma_{(1,3)}$ (i.e., at $t=\tau$) we apply the K map to $\Gamma_{(2)}$ generating $M^{(K)}\Gamma_{(2)}\equiv\Gamma_{(5)}$. (Note that we denote the trajectory τ segment $\Gamma_{(i)}\to\Gamma_{(j)}$, segment $\Gamma_{(i,j)}$.) If we now reverse time keeping the same shear rate, we obtain $\Gamma_{(4)}=\exp[-iL(\Gamma_{(5)},\gamma)\tau]\Gamma_{(5)}$. $\Gamma_{(4)}$ is the initial $t=0$ phase from which a segment $\Gamma_{(4,6)}$ can be generated with $\Gamma_{(6)}=\exp[iL(\Gamma_{(4)},\gamma)2\tau]\Gamma_{(4)}$.

We now show that segments $\Gamma_{(1,3)}$ and $\Gamma_{(6,4)}$ are conjugate. Using the symmetry of the equations of motion it is trivial to show that $P_{xy}(\Gamma_{(2)})=-P_{xy}(\Gamma_{(5)})$ and, from Eq. (7), that $P_{xy}(t;\Gamma_{(1)},0<t<2\tau)=-P_{xy}(2\tau-t;\Gamma_{(6)},0<t<2\tau)$. Thus $\Gamma_{(1,3)}$ is the conjugate segment of $\Gamma_{(6,4)}$ and $\langle P_{xy}\rangle_{\tau,(6,4)}=-\langle P_{xy}\rangle_{\tau,(1,3)}$. We now have an algorithm for finding *initial* phases which will subsequently generate the conjugate segments [5]. These trajectory segments and mappings are illustrated in Fig. 1 where $\tau=2$.
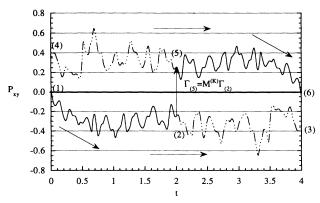
We now discuss the ratio of probabilities of finding the

FIG. 1. P_{xy} for trajectory segments from a simulation of 200 disks at $T = \sum_i p_i^2/2mNk_B = 1.0$ and $n = N/V = 0.4$. The trajectory segment $\Gamma_{(1,3)}$ was obtained from a forward time simulation. At $t = 2$, a K map was applied to $\Gamma_{(2)}$ to give $\Gamma_{(5)}$. Forward and reverse time simulations from this point give the trajectory segments $\Gamma_{(5,6)}$ and $\Gamma_{(5,4)}$, respectively. If one inverts P_{xy} in $P_{xy} = 0$ and inverts time about $t = 2$, one transforms the $P_{xy}(t)$ values for the antisegment $\Gamma_{(4,6)}$ into those for the conjugate segment $\Gamma_{(1,3)}$.

initial phases $\Gamma_{(1)}, \Gamma_{(4)}$ which generate these conjugate segments. The probabilities of observing the segments $\Gamma_{(1,3)}, \Gamma_{(4,6)}$ are of course proportional to the probabilities of observing the initial phases which generate those segments. It is convenient to consider a small phase space volume $V(\Gamma_{(i)}(0))$ about an initial phase $\Gamma_{(i)}(0)$. Because the initial phases are distributed *microcanonically*, the probability, of observing ensemble members inside $V(\Gamma_{(i)}(0))$ is proportional to $V(\Gamma_{(i)}(0))$. From the Liouville equation $df(\Gamma, t)/dt = 3N\alpha(\Gamma)f(\Gamma, t) + O(1)$ and the fact that for sufficiently small volumes $V(\Gamma(t)) \sim 1/f(\Gamma(t), t)$, we can make the following observations: $V_2 = V_1(\tau) = V_1(0)\exp[-\int_0^\tau 3N\alpha(s; \Gamma_{(1)})ds]$ and $V_3 = V_1(2\tau) = V_1(0)\exp[-\int_0^{2\tau} 3N\alpha(s; \Gamma_{(1)})ds]$.

Because the segment $\Gamma_{(4,6)}$ is related to $\Gamma_{(1,3)}$ by a K map, which is applied at $t = \tau$, and the Jacobian of the K mapping is unity, $V_2 = V_5$, $V_3 = V_4$, and $V_1(0) = V_6$.

However, since $V_1(0)$ and V_4 are volumes at $t = 0$ and since the distribution of initial phases is microcanonical, we can compute the ratio of probabilities of observing $t = 0$ phases within $V_1(0)$ and V_4. This ratio is just the volume ratio

$$\mu_{1*}/\mu_1 = V_4/V_1(0) = V_1(2\tau)/V_1(0)$$

$$= \exp\left[\int_0^{2\tau}(-3)N\alpha(s; \Gamma_{(1)})ds\right],$$

$$\forall \tau. \quad (8)$$

This is the same result as that deduced from (2), except that the segment length is 2τ rather than τ and the ratio of probabilities is valid for arbitrary τ rather than just in the asymptotic $\tau \to \infty$ limit as is the case in [2].

Thus if $\langle \alpha \rangle_{\tau,(1,3)}$ is positive, it becomes exponentially probable that states sampled at equilibrium will subsequently generate segments rather than antisegments, i.e., $\lim_{\tau \to \infty} V_4/V_1(0) = 0$. [Note that if we assume $\langle \alpha \rangle_{\tau,(2,3)} < 0$, the same conclusion is obtained since V_4 is then the segment producing initial volume and

$\lim_{\tau \to \infty} V_4/V_1(0) = \infty$.] The measure of antisegment generating initial phases vanishes exponentially with the duration τ of the segment.

We decided to test Eq. (8) for the probability ratio of observing transient segments and antisegments by performing numerical simulations. We carried out molecular dynamics simulations of $N = 50$ and 200 disks in two Cartesian dimensions. The disks were characterized by simple short ranged pair potential $\phi(r)$, which is, in reduced units [1,2,6]

$$\phi(r) = \begin{cases} 4[r^{-12} - r^{-6}] + 1 & \text{for } r < 2^{1/6} \\ 0 & \text{for } r > 2^{1/6}. \end{cases} \quad (9)$$

In reduced units the particle mass is unity. Shearing periodic boundary conditions were used to minimize boundary effects [1].

In Fig. 1 we show $P_{xy}(t)$ for a single trajectory segment of length $\tau = 2.0$ and its mappings. The initial phase was selected from an equilibrium distribution and a strain rate of unity was applied to the system at $t = 0$. The simulation was carried out at a constant kinetic temperature, $T = \sum_i p_i^2/2mNk_B$ of 1.0 with $N = 200$ and $n = N/V = 0.4$. At $t = 2$, a K map was applied, enabling the construction of the antisegment $\Gamma_{(4,6)}$ from its conjugate segment, namely, $\Gamma_{(1,3)}$, as described above.

If one looks at the results in Fig. 1 very closely one can see that if the segment $\Gamma_{(1,3)}$ is time reversed and inverted in $P_{xy} = 0$, then one obtains the segment $\Gamma_{(4,6)}$, exactly as predicted above from the symmetry of the equations of motion. One can also see if one inspects the results in detail that the accuracy of the calculations is such that these calculations are time reversible over the time scale shown in the figure. Numerical integration accuracy is not an issue for the time scales shown in this figure. Further, these time scales are *much* longer than the Maxwell time for this system.

Figure 2 shows the time evolution of the phase space volume ratio [7] $V_{i(K)}(2\tau)/V_i(0) = V_i(2\tau)/V_i(0) = \exp[\int_0^{2\tau}(-1)(2N-3)\alpha(s; \Gamma_{(i)})ds]$ for four different typical initial equilibrium phases $\Gamma_{(i)}$. The data are plotted for a constant internal energy $H_0/N = 1.091\,61$ system for $N = 200$, $n = N/V = 0.4$, and $\gamma = 1.0$ for τ up to 0.1. The volume ratios were computed by taking the ex-
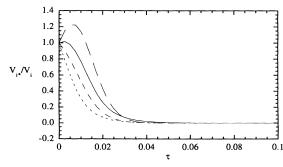

FIG. 2. The time evolution of the volume ratio V_{i*}/V_i for four different typical initial equilibrium phases from a constant internal energy simulation of 200 disks at $H_0/N = 1.091\,61$, $n = N/V = 0.4$, and $\gamma = 1.0$.

ponential of the time integral of α for each of the trajectory segments. Note that the computed volume ratios do not necessarily decay to zero monotonically. For a short period of time near $t=0$ the volume ratio actually increased for two of the trajectory segments. Equation (8), however, predicts that as time increases it will become overwhelmingly likely that the segments satisfy the second law and therefore have $\langle \alpha \rangle_{t,(1,3)}>0$ and an exponential decay of the volume ratio to zero. This is observed for each of these segments.

In Fig. 3 we directly compute the ratio of probabilities of seeing transient trajectory segments and their conjugates. These probabilities were found by generating transient shearing trajectories from a set of phases sampled from the equilibrium microcanonical distribution. The probabilities were estimated by histogramming the segments according to their value of $A(2\tau) \equiv \int_0^{2\tau} \alpha(s)ds$, the time integrated entropy production per degree of freedom.

In Fig. 3 we plot $\ln\Pi(2\tau) \equiv \ln[p(A(2\tau))/p(-A(2\tau))]$ for a system where $N=50$, $\tau=0.5$, $H_0/N=0.907$, and there is a shear rate of 0.1. As can be seen from the figure, this function is essentially linear in $A(2\tau)$. The straight line shows a weighted least-squares fit to the observed logarithmic probability ratio which has a slope of 95 ± 2, in agreement with the value of the slope predicted from the ratio of phase space volumes, namely, $2N-3=97$ [7]. Thus the ratio of probabilities of observing segments to that of observing antisegments is in numerical agreement with the prediction of (8).

In summary, the use of symmetry properties of the reversible equations of motion has enabled us to predict the relative probability of sampling at equilibrium, phases which will subsequently generate segments and antisegments. We have shown that it becomes exponentially probable that initial phases will generate second law satisfying segments rather than their time reversed conjugates, namely, antisegments. This anisotropic probability ratio results from the fact that the measure of those phases which will generate second law violating trajectories vanishes exponentially with time.

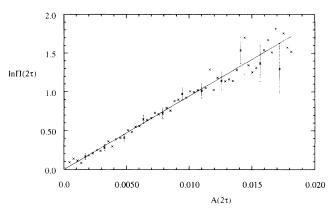The expression we derive (8) for this ratio of probabili-

FIG. 3. The logarithmic probability ratio of observing segments and antisegments $\ln\Pi \equiv \ln[p(A(2\tau))/p(-A(2\tau))]$ as a function of the integrated entropy production per degree of freedom $A(2\tau)$. The data were obtained by histogramming observed segment frequency data from a simulation of 50 disks where $H_0/N=0.907$, $n=N/V=0.4$, and $\gamma=0.1$. The straight line is a weighted least-squares fit to the data and has a slope of 95 ± 2.

ties is identical to that we recently derived [Eq. (2)], not for transient trajectory segments but rather for steady state trajectory segments, using our recently defined natural invariant measure for steady states. The present work thus confirms the validity of both the invariant measure introduced in [2] and the application (8) to steady states as derived in [2]. It is remarkable that the invariant measure which deals in the steady state only with *expanding* Lyapunov eigenvalues leads to the same result as that predicted from the present considerations of transients and which involves both the expanding and contracting eigenvalues. [Equation (8) involves the thermostat multiplier and through (3) the sum of all Lyapunov exponents.] Thus although our present geometrical argument is not directly related to mechanical stability, it is clear that there is a deep connection between the two.

[1] D. J. Evans and G. P. Morriss, *Statistical Mechanics of Nonequilibrium Liquids* (Academic, London, 1990).

[2] D. J. Evans, E. G. D. Cohen, and G. P. Morriss, Phys. Rev. Lett. **71**, 2401 (1993).

[3] This measure, proposed in [2], was developed in the spirit of measures used for cycle expansions: W. N. Vance, Phys. Rev. Lett. **69**, 1356 (1992); P. Cvitanovic, P. Gaspard, and T. Schreiber, Chaos **2**, 85 (1992); R. Artuso, E. Aurell, and P. Cvitanovic, Nonlinearity **3**, 325 (1990), and references therein; P. Gaspard and F. Baras, in *Microscopic Simulations of Complex Hydrodynamic Phenom-*

ena, Vol. 292 of *NATO Advanced Study Institute, Series B: Physics*, edited by M. Mareschal and B. L. Holian (Plenum, New York, 1991).

[4] J.-P. Eckmann and D. Ruelle, Rev. Mod. Phys. **57**, 617 (1985).

[5] Note that the conjugate segment is unique.

[6] J. D. Weeks, D. Chandler, and H. C. Andersen, J. Chem. Phys. **54**, 5237 (1971).

[7] This is the corrected version of (8) for a two dimensional fluid including terms of $O(1/N)$.